

Copper Complexes in the Promotion of Aldol Addition to Pyridine-2-carboxaldehyde: Synthesis of Homo- and Heteroleptic Complexes and Stereoselective Double Aldol Addition

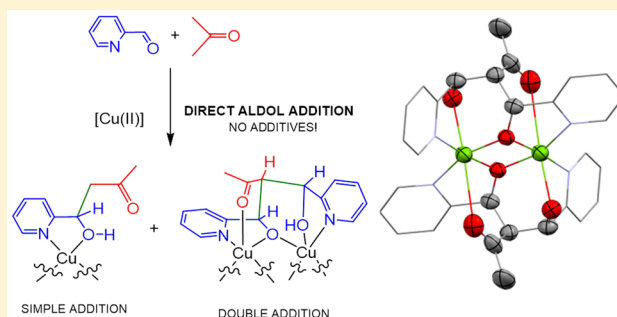
Lucía Álvarez-Miguel,[†] Héctor Barbero,[†] Adriana Sacristán-Martín,[†] José M. Martín Álvarez,[†] Alfonso Pérez-Encabo,[‡] Celedonio M. Álvarez,[†] Raúl García-Rodríguez,^{*,†} and Daniel Miguel^{*,†}

[†]GIR MIOMeT/IU CINQUIMA/Química Inorgánica, Facultad de Ciencias, Universidad de Valladolid, Paseo de Belén 7, E-47011 Valladolid, Spain

[‡]IU CINQUIMA/Química Orgánica, Facultad de Ciencias, Universidad de Valladolid, Paseo de Belén 7, E-47011 Valladolid, Spain

Supporting Information

ABSTRACT: $\text{CuCl}_2 \cdot 2\text{H}_2\text{O}$ and $\text{Cu}(\text{ClO}_4)_2 \cdot 6\text{H}_2\text{O}$ are able to promote aldol addition of pyridine-2-carboxaldehyde (pyca) with acetone, acetophenone, or cyclohexenone under neutral and mild conditions. The general and simple one-pot procedure for the aldol addition to $\text{Cu}(\text{II})$ complexes accesses novel Cu complexes with a large variety of different structural motifs, from which the aldol-addition ligand can be liberated by treatment with NH_3 . Neutral heteroleptic complexes in which the ligand acts as bidentate, or homoleptic cationic complexes in which the ligand acts as tridentate can be obtained depending on the copper salt used. The key step in these reactions is the coordination of pyca to copper, which increases the electrophilic character of the aldehyde, with $\text{Cu}(\text{ClO}_4)_2$ leading to a higher degree of activation than CuCl_2 , as predicted by DFT calculations. A regio- and stereoselective double aldol addition of pyca in the reaction of $\text{Cu}(\text{ClO}_4)_2 \cdot 6\text{H}_2\text{O}$ with acetone leads to the formation of a dimer copper complex in which the novel double aldol addition product acts as a pentadentate ligand. A possible mechanism is discussed. The work is supported by extensive crystallographic studies.

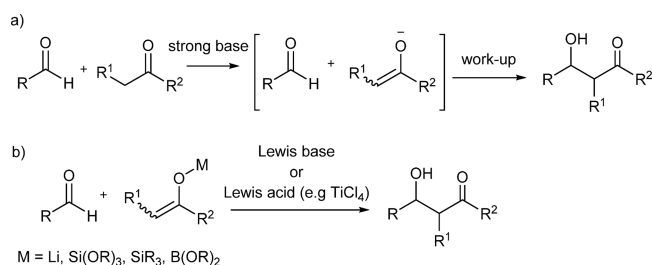


INTRODUCTION

Copper is a cheap and ubiquitous metal and one of the most abundant transition metals present in living systems. It is very active in promoting a large number of catalytic and stoichiometric transformations due to its Lewis acid character and its redox activity, which makes the use of copper complexes very attractive in modern organic chemistry.¹ In particular, copper is able to promote C–C and C–heteroatom bond formation through aldol addition and related processes, and it has been extensively used, together with chiral ligands, in the catalytic enantioselective synthesis of chiral molecules.²

Aldol reactions are among the most powerful tools for the creation of C–C bonds.^{3,4} The popularity of this reaction stems from the large library of protocols available, which allows the chemist great control and selectivity over the final product. In these reactions, an enolizable carbonyl compound with acidic hydrogens in the α position acts as a nucleophile toward an electrophilic carbonyl, typically an aldehyde or ketone (see Scheme 1a). The control in aldol addition relies on the choice of the enolizable carbonyl and the carbonyl electrophile precursor. Depending on the strategy chosen, it is possible to obtain different chemoselective, regioselective, diastereoselective, and enantioselective aldol products.^{3,5} Despite providing a great level of control, existing methods rely on the use of additives, usually

Scheme 1. (a) General Aldol Addition under Strongly Basic Conditions. (b) Aldol Reaction via Preformed Enolates



accompanied by strongly basic or acidic conditions. For instance, strong bases such as LDA are normally used to generate the lithium enolate. For the formation of silicon and boron enolates, additional reagents, such as TMSCl or expensive dialkylboron triflate, are required. The “preformed” enolate subsequently reacts with the carbonyl electrophile, usually in the presence of a Lewis base or a Lewis acid (typically TiCl_4) that enhances its electrophilic character (see Scheme 1b).^{5b,6}

Received: September 24, 2017



Considerable efforts have gone into developing methods for the “direct” aldol reaction, in which the compounds undergoing reaction are activated “in situ” to avoid the preparation of a “preformed” enolate in a separate step, as well as into finding more tolerant Lewis acids capable of activating the carbonyl in milder conditions.⁷ Since the seminal work by Evans,⁸ in which the enantioselective addition of silyl enolates to (benzyloxy)-acetaldehydes, which act as chelating electrophiles, was achieved using a chiral Cu(II) catalyst, a large number of copper(II) complexes have emerged as convenient catalysts for the aldol reaction.⁹ Despite the large number of examples of Cu(II) complexes employed in the aldol addition, most methodologies are based on preactivated silyl enolates; comparatively few examples of the use of Cu(II) complexes in the direct aldol^{2a,e,10} or nitro-aldol¹¹ reaction are known. For instance, Cu(II) complexes derived from ortho substituted pyridine ligands have been shown to be highly efficient catalysts in the direct asymmetric aldol reactions of ketones while keeping very good stereoselectivity.^{10e,f}

In light of the wide use of Cu(II) in catalysis, the formation of copper complexes with molecules derived from aldol addition has been relatively less explored, and there is still a lack of general protocols available to access such compounds.¹² Given the great structural diversity of Cu(II) complexes, the study of the structures of Cu(II)-aldol ligand complexes could also be beneficial to the understanding of the exact catalytic mechanisms. Recently, a few examples of self-aldol type reactions in which the product remains coordinated to copper as a ligand in the coordination sphere of copper(II) have been published; however, these required strongly basic conditions.¹³

In the course of our previous studies of the Schiff condensation reactions of pyridine-2-carboxaldehyde (pyca) with peptides and other molecules,¹⁴ we found some very interesting examples of the addition of acetone to pyca in manganese(I) and rhenium(I) carbonyl systems.¹⁵ These reactions required the previous coordination of pyca to the metal complex (by thermally induced carbonyl substitutions) and the use of an appropriate halogen extractor reagent in order to create a coordination vacancy. Cu(II) complexes such as CuCl₂ and Cu(ClO₄)₂ are harder Lewis acids that have several available coordination sites and flexible coordination geometries as a result of the d⁹ configuration. We anticipated that the ability of copper(II) to promote aldol addition could be exploited to design simple methods for the preparation of complexes containing mixed N,O donors derived from the aldol additions of ketones to pyca. Our approach, although a simple one, echoes the way that class II aldolases are used in nature, which has inspired the development of several small molecule catalysts.¹⁶ Class II aldolases use as a cofactor a transition metal that acts as a Lewis acid (typically Zn²⁺, although other divalent transition metals such as Fe²⁺ or Co²⁺ are known).¹⁷ Bidentate coordination of the carbonyl substrate acidifies the α -protons, so that the resulting metal enolate can subsequently attack a hydrogen-bonding activated carbonyl to give the aldol product upon decomplexation. We envisioned that the use of pyca as chelate ligand would promote the activation of the electrophile through strong bidentate coordination to Cu(II), while the presence of additional binding sites would be used to simultaneously acidify the α -protons of the ketone, thus facilitating the formation of the enolate (see Figure 1).

Our aim herein is to explore the possibility of using cheap and easily available Cu(II) sources under aerobic and neutral conditions to promote aldol reaction with several objectives in

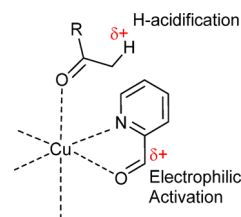


Figure 1. Scheme of the synthetic approach for the in situ aldol addition promoted by Cu(II).

mind: (i) To devise facile and simple procedures for the preparation of complexes containing mixed N,O ligands via in situ aldol addition to Cu(II) complexes, including the subsequent liberation of the aldol product from the complex. (ii) To study the dependence of the reactivity patterns on the Cu(II) source employed. Additionally, we report a novel and stereoselective double aldol addition of acetone to pyca. The work is supported by extensive crystallographic analyses of the complexes.

RESULTS AND DISCUSSION

We started our studies with the one-pot reaction of CuCl₂·2H₂O with 1 equiv of pyridine-2-carboxaldehyde (pyca) in acetone, in order to assess whether the copper complex could promote the aldol addition under mild conditions. After 10 h at room temperature, green microcrystals of **1a** were obtained in virtually quantitative yield (92%). The structure of **1a** was studied by X-ray crystallography, revealing that complex **1a** contains a κ^2 (N,O) hydroxyketone ligand (*HL1a*) that results from the aldol addition of acetone to the aldehyde carbon of pyca (see Figure 2 and Scheme 2). The coordination around copper is

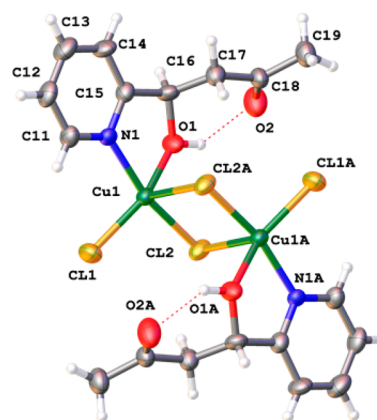
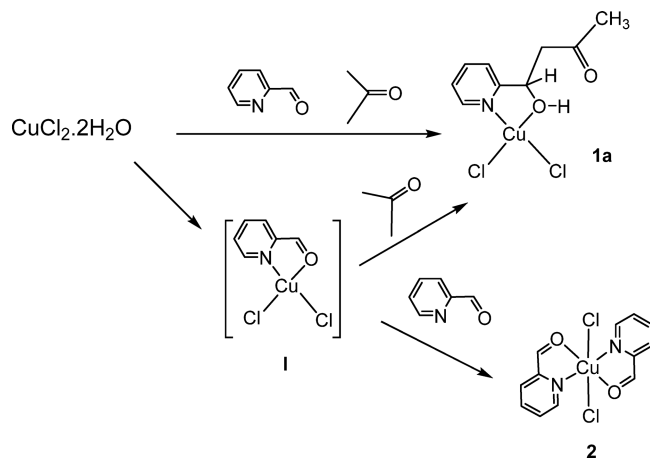


Figure 2. Structure of **1a** showing the association into dimers in solid state through Cu–Cl interactions. Selected bond lengths (Å) and angles (deg): Cu(1)–Cl(1) 2.216(2), Cu(1)–Cl(2) 2.254(1), Cu(1)–Cl(2A) 2.757(2), Cu(1)–N(1) 2.008(4), Cu(1)–O(1) 1.996(3), N(1)–Cu(1)–O(1) 78.40(0), Cl(1)–Cu(1)–Cl(2) 96.45(6), Cl(2)–Cu(1)–Cl(2A) 91.72(5). H-Bonding: O(1)–H(1) 0.938(0), O(1)···O(2) 2.679(4), H(1)···O(2) 1.945(4), O(1)–H(1)···O(2) 133.5(3).

completed by two chloride ligands, forming a nearly planar arrangement around the copper atom. In the solid state, the molecules are arranged in the lattice to form centrosymmetric dimers through longer Cu–Cl interactions of 2.756(2) Å, as shown in Figure 2, and therefore, the copper atom can be considered to lie in a nearly square pyramidal pentacoordinated environment, in which the Addison parameter (τ) is 0.18.¹⁸ The quantitative formation of **1a** from CuCl₂ is quite remarkable

Scheme 2. Reaction of $\text{CuCl}_2 \cdot 2\text{H}_2\text{O}$ with Pyridine-2-carboxaldehyde (pyca) To Give Complex 1a, Featuring the $\kappa^2(\text{N},\text{O})$ Hydroxyketone Ligand (*HL1a*) That Results from the *in Situ* Aldol Addition of Acetone to pyca^a



^aThe reaction involves the intermediacy of a complex in which pyca coordinates to CuCl_2 in a chelate fashion (I). Although this complex could not be isolated, addition of an excess of pyca resulted in the precipitation of complex 2, thus demonstrating the coordination of pyca as a chelate to Cu.

since it shows the ability of the copper complex to promote the aldol addition of acetone to the pyca aldehyde in the absence of a base and under mild conditions. Although the high thermodynamic stability of the resulting complex is usually the driving force for the formation of the ligand in the coordination sphere of the metal, it may make the liberation of the ligand difficult.^{13,15} Therefore, we moved next to test whether the hydroxyketone ligand derived from the aldol addition of acetone to pyca (*HL1a*) could be liberated from complex 1a. To our delight, we found that this task can be easily accomplished by simple treatment of the complexes with $\text{NH}_3/\text{CH}_2\text{Cl}_2$ (see the [Experimental Section](#)), which resulted in the easy liberation and isolation of the pyridyl ligand *HL1a* from the complex 1a.

A possible reaction pathway for the formation of complex 1a would involve initial coordination of one molecule of pyca as a chelate $\kappa^2(\text{N},\text{O})$ to CuCl_2 to give an intermediate complex I in which the electrophilic character of the aldehyde is increased, favoring the attack of the acetone enolate to give 1a (Scheme 2). The coordination sphere of I is not saturated, so a molecule of acetone could additionally interact with the complex, increasing the acidity of the α -hydrogen atoms of the ketone.^{17a} This further facilitates the attack to the activated pyca aldehyde so that the aldol reaction occurs under mild and neutral conditions to give complex 1a. All attempts to produce a second aldol addition by reacting 1a with 1 equiv of pyca and acetone did not work; unreacted 1a was recovered in all cases. This is perhaps not surprising since the coordination and activation of a second molecule of pyca and acetone are compromised due to the presence of the pyridyl hydroxyketone ligand *HL1a* and the two chloride ligands.

Although attempts to isolate any intermediate from the reaction mixture have failed so far, the reaction of $\text{CuCl}_2 \cdot 2\text{H}_2\text{O}$ in acetone with an excess of pyridine-2-carboxaldehyde (3 equiv) results in the clean precipitation of complex 2 after 15 min, which can be isolated in virtually quantitative yield (95%). Figure 3 shows the structure of compound 2, which contains two molecules of pyca coordinated in a chelating fashion to copper

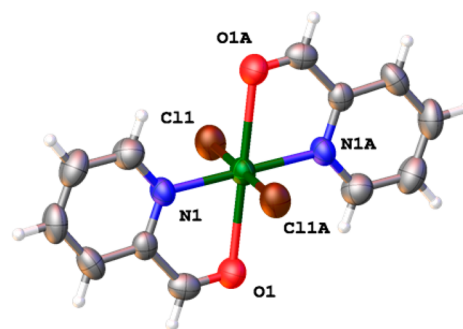


Figure 3. Perspective view of compound 2 showing the atom numbering. Selected bond lengths (Å) and angles (deg): Cu(1)–Cl(1) 2.299(1), Cu(1)–N(1) 1.989(4), Cu(1)–O(1) 2.443(4), Cl(1)–Cu(1)–Cl(1A) 180.00(1), Cl(1)–Cu(1)–N(1) 90.80(15), Cl(1)–Cu(1)–O(1) 90.80(15).

through the nitrogen atom of the pyridine ring and the oxygen atom of the aldehyde group as a $\kappa^2(\text{N},\text{O})$ chelate. The structure of 2 can be considered octahedral, although the Cu–O distances of 2.443(4) Å are somewhat long for a normal Cu–O bond, which is consistent with the Jahn–Teller distortion expected for the $\text{Cu}(\text{II})$ d^9 ion.

IR spectroscopy shows a decrease of 82 cm^{-1} for the $\nu(\text{CO})$ band of the coordinated aldehyde in 2 with respect to the free pyridine-2-carboxaldehyde (1631 cm^{-1} vs 1713 cm^{-1}), showing that the aldehyde has a more electrophilic character as a result of the coordination of pyca to Cu. To further support that idea, we performed DFT calculations (a Natural Population Analysis, NPA; see Figure 4). These calculations show that the charge on

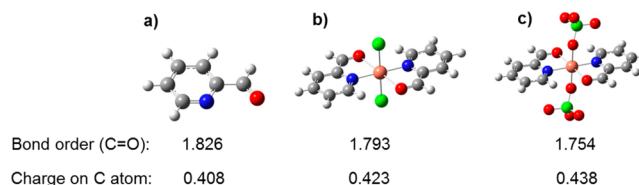
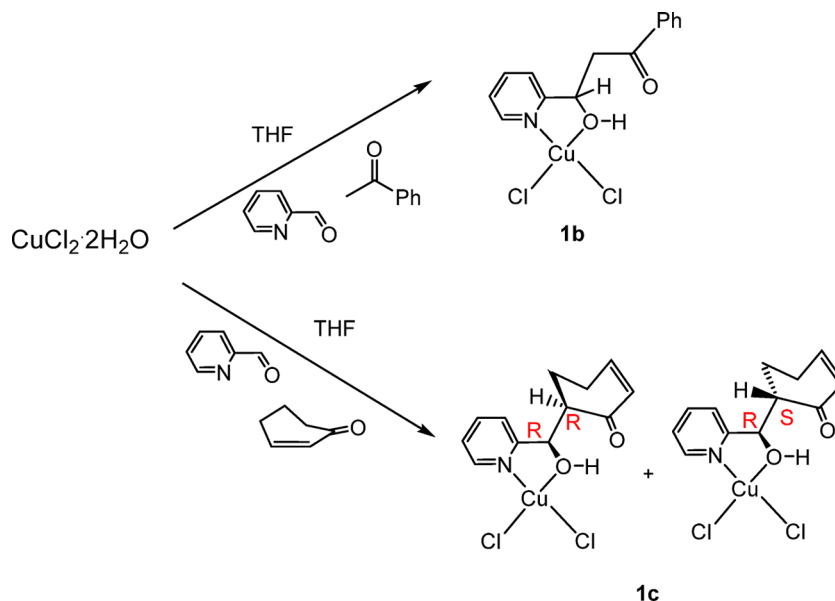


Figure 4. Optimized geometries, bond orders, and charge on the aldehyde carbon atom obtained from DFT calculations for (a) free pyca; (b) $\text{CuCl}_2(\text{pyca})_2$, complex 2; and (c) $\text{Cu}(\text{ClO}_4)_2(\text{pyca})_2$.

the C atom increases from +0.408 on the isolated pyca ligand (Figure 4a) to +0.423 when the pyca ligand is coordinated to Cu as in compound 2 (Figure 4b), as well as a decrease in the bond order from 1.826 to 1.793, thus supporting the key role of the coordination of pyca to copper in the activation of the aldehyde bond for the aldol addition. An obvious and easy way to vary the degree of activation of the pyca ligand is through the ligands present in the complex. We reasoned that the use of more electron deficient complexes of copper would result in a greater degree of activation for the pyca ligand. In order to further explore this perspective, we carried out similar DFT calculations on the ClO_4 analogue of 2 (see Figure 4c). This shows that simply changing the chloride for perchlorate in the coordination sphere of the metal leads to a higher degree of activation for the aldehydic ligand, as reflected by a further decrease in bond order with respect to the free ligand (from 1.826 to 1.754), making additional coordination sites in the metal possible, and thus opening the possibility of novel reactivities (see later discussion).

We next moved to study the use of this methodology for the aldol addition of different ketones in order to further understand

Scheme 3. Copper(II) Complexes with Pyridine-2-carboxaldehyde, and Aldol Addition of Acetophenone and Cyclohexenone^a

^aFor the latter, a mixture of diastereoisomers (70/30) is found.

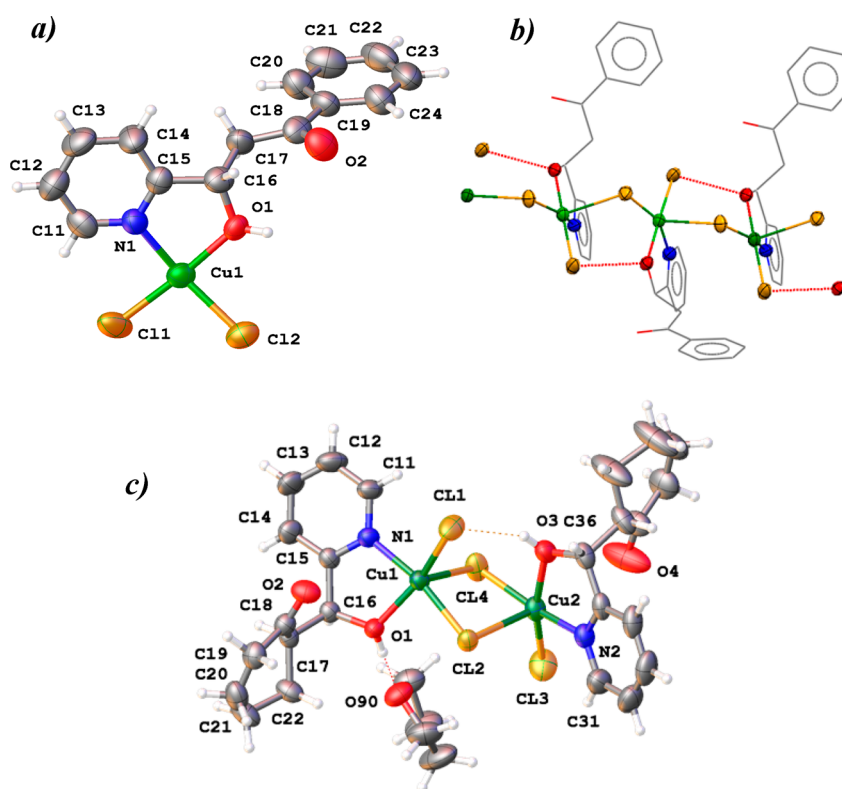


Figure 5. (a) Structure of **1b** showing the atom numbering. Selected bond lengths (Å) and angles (deg): Cu(1)–Cl(2) 2.260(2), Cu(1)–Cl(1) 2.255(2), Cu(1)–Cl(1A) 2.741(2), Cu(1)–N(1) 2.016 (6), Cu(1)–O(1) 2.009(5), N(1)–Cu(1)–O(1) 80.0(2) Cl(1)–Cu(1)–Cl(2) 95.75(8), Cl(1)–Cu(1)–Cl(1A) 91.71 (7). H-Bonding: O(1)–H(1) 0.938(0), O(1)⋯O(2) 3.205(8), H(1)⋯O(2) 2.696(6), O(1)–H(1)⋯O(2) 114.9(4). (b) Polymeric structure of **1b** through Cl(2)⋯Cu(1) interactions between adjacent complexes, so that the geometry around Cu can be considered square pyramidal. (c) Structure of **1c** showing the atom numbering. Selected bond lengths (Å) and angles (deg): Cu(1)–Cl(1) 2.225(2), Cu(1)–Cl(2) 2.259(1), Cu(1)–Cl(4) 2.756(1), Cu(1)–N(1) 1.996 (3), Cu(1)–O(1) 2.036(3), Cu(1)–Cu(2) 3.5597(7), N(1)–Cu(1)–O(1) 80.42(13) Cl(1)–Cu(1)–Cl(2) 97.33(5), Cl(2)–Cu(1)–Cl(4) 87.06 (4). H-Bonding: O(1)–H(1) 0.938(0), O(1)⋯Cl(3) 3.092(3), H(1)⋯Cl(3) 2.205(1), O(1)–H(1)⋯Cl(3) 157.3(2), O(3)–H(3) 0.938(0), O(3)⋯O(90) 2.565(4), H(3)⋯O(90) 1.640(3), O(3)–H(3)⋯O(90) 168.1(2).

this reactivity and explore the scope of this reaction. We selected acetophenone and cyclohexenone. The latter was selected because its only enolizable α -carbon atom is prochiral, and

therefore, we could evaluate whether the metal center could induce stereoselectivity, since it is known that subtle interactions may induce large stereochemical effects.¹⁹ The general procedure

Scheme 4. Deprotonation of the Hydroxyl Group of Complexes **1a–b** To Give Alkoxo-Bridged Dimers **3a–b**, Containing the Anionic Ligands **L1a[−]** and **L1b[−]**

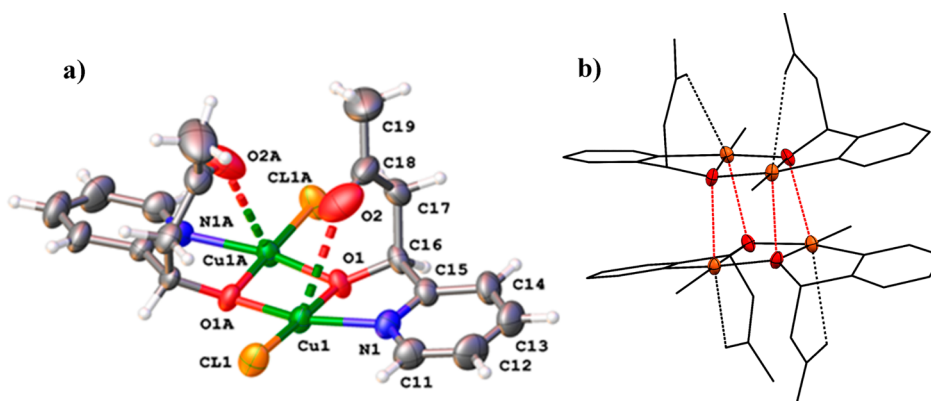
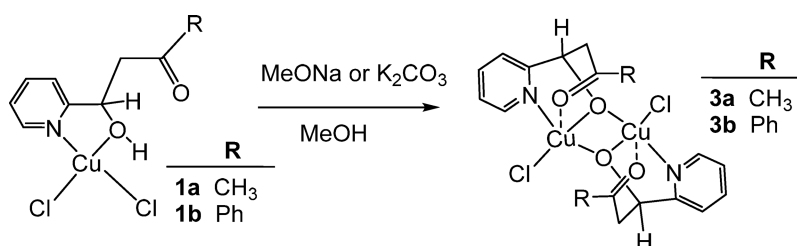


Figure 6. (a) Structure of **3a**, showing the atom numbering. Selected bond lengths (Å) and angles (deg): Cu(1)–N(1) 1.988(2), Cu(1)–O(1) 1.929(2), Cu(1)–O(2) 1.954(2), O(1)–Cu(1)–N(1) 81.46(9), O(1)–Cu(1)–O(1A) 78.32(8), Cl(1)–Cu(1)–N(1) 99.47(7). (b) Interaction of the two Cu_2O_2 rings through the alkoxide (highlighted in red) to give an overall octahedral geometry around each Cu center and the formation of a Cu_4O_4 central cage.

is a simple one, which consists of simply mixing CuCl_2 , pyca, and the corresponding ketone in THF at room temperature (see Scheme 3). In this way, the corresponding complexes **1b** and **1c** resulting from the aldol addition of acetophenone and cyclohexenone were prepared in 84% and 86% yield after 16 h at room temperature, respectively. The structure of complexes **1b** and **1c** was determined crystallographically, confirming the aldol addition to the pyca aldehyde and the formation of the novel pyridyl aldol ligands in the coordination sphere of copper, as shown in Figure 5.

The free pyridyl aldol ligands **HL1b** and **HL1c** were easily liberated from complexes **1b** and **1c**, respectively, and isolated as an oil (**HL1c**) or in crystalline form (**HL1b**). For the latter, the integrity of the ligand was confirmed by X-ray diffraction (see the SI). NMR studies of the reaction crude of **1c** showed the formation of 2 isomers in a 70/30 ratio. This result is not surprising since, in principle, the aldol reaction could occur through either of the two faces of the enolate, thus leading to the formation of two diastereoisomers, each of them present as a pair of enantiomers (SS/RR and RS/SR). Although both diastereoisomers are formed in the reaction, the X-ray structure obtained for complex **1c** (Figure 5c) contains only the RS/SR ligand **HL1c** (which is present as pair of enantiomers in the crystal). Figure 5 shows the structures of complexes **1b** and **1c**. In both structures, the coordination environment around copper can be viewed as square pyramidal ($\tau = 0.052$ for **1c**) or distorted square pyramidal ($\tau = 0.35$ for **1b**) in which the newly generated ligand acts as a κ^2 (N,O) chelate through the nitrogen of the pyridine and the OH group, as observed for **1a**. However, the structures exhibit some notable differences. Compound **1c** (Figure 5c) shows the formation of chloride bridged dimers thorough $\text{Cl}\cdots\text{Cu}$ interactions, similar to **1a** but with the

difference that now the two OH groups are not engaged in intramolecular hydrogen bonds with the $\text{C}=\text{O}$ group but instead form intermolecular $\text{O}\cdots\text{H}\cdots\text{O}(\text{THF})$ and $\text{OH}\cdots\text{Cl}$ hydrogen bonds. In sharp contrast, compound **1b** (Figure 5b) forms a one-dimensional polymeric chain in which the structure propagates indefinitely through longer $\text{Cl}(2)\cdots\text{Cu}(1)$ interactions at 2.741(2) Å (cf. intramolecular $\text{Cl}(2)\cdots\text{Cu}(1)$ 2.260(2) Å) as shown in Figure 5b. Additionally, there is an intermolecular H-bond between the hydroxyl group and the terminal chlorine atom of the next molecule, instead of the intramolecular $\text{O}\cdots\text{H}\cdots\text{O}(\text{ketone})$ observed in the structure of **1a** (Figure 2). The extent to which these secondary interactions and H bonds contribute to the observed differences in the solid phase arrangement (dimer vs polymer) is unclear at this stage.

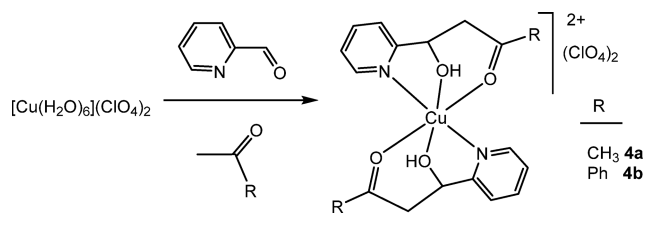
The coordination of the pyridyl hydroxyketone ligand in complexes **1a–c** to copper through the OH group (see above) should promote the easy removal of the hydroxyl proton. Indeed, treatment of **1a** and **1b** with K_2CO_3 or MeONa in MeOH leads to the clean deprotonation of the hydroxyl group to give the anionic ligands **L1a[−]** and **L1b[−]** and the precipitation of dimers **3a** and **3b** (Scheme 4) in excellent yields (92–94%; see the Experimental Section). The structure determination of **3a** confirmed the deprotonation of the OH group and subsequent concerted substitution of chloride on another molecule, leading to the formation of dimers in which the alkoxide bridge brings the two Cu atoms together in a central Cu_2O_2 ring unit (Figure 6a). The ketonic oxygen, which, in the starting **1a**, was H-bonded to the hydroxyl, now forms a loose bond ($\text{Cu}(1)\cdots\text{O}(2)$ 2.934(3) Å) with copper. In addition to this, the alkoxide group also forms an additional weak interaction $\text{Cu}(1)\cdots\text{O}(2)$ 2.674(2) Å between dimers bringing together two Cu_2O_2 cores to provide

an overall distorted octahedral geometry around the copper atom (Figure 6b).

It is worth mentioning that the deprotonation of the complex **1a** can also occur after prolonged storage in solution and in the absence of a base. Storage of compound **1a** in methanol at room temperature yielded the formation of a few crystals of **3a** after 48 h. This result illustrates not only the increased acidity of the hydroxyl groups as a result of the coordination to copper but also the ability of the alkoxo/OH ligand to form bridges. As described above, the success of the aldol reaction promoted by CuCl_2 seems to involve several factors. First, coordination of pyca to copper enhances the electrophilic character of the aldehyde, and second, the Cu(II) atom increases the acidity of the α -hydrogen atoms of the ketone in such a way that aldol addition occurs under mild conditions.

With this background in mind, we decided to explore the use of $\text{Cu}(\text{ClO}_4)_2 \cdot 6\text{H}_2\text{O}$ in the aldol addition. Replacing Cl^- with ClO_4^- results in an increase of the Lewis acidity of Cu, which in turn leads to a higher degree of activation for the pyca aldehyde, as shown by DFT calculations (see above, Figure 4). In addition to this, the choice of a much less coordinating ligand (ClO_4^- instead of Cl^-) not only opens up more coordination sites but should also enhance the activation of the ketone by interacting with Cu, which is now more available for coordination. To test these ideas, we reacted $\text{Cu}(\text{ClO}_4)_2 \cdot 6\text{H}_2\text{O}$ and pyca with acetone or acetophenone at room temperature in THF (Scheme 5). The

Scheme 5. Aldol Addition of Acetone to pyca in Cationic Cu(II) Complexes



reaction resulted in the fast (cf 10 h for **1a** vs 4 h for **4a**) formation of cationic homoleptic complexes **4a** and **4b** that are now formed by the coordination of two ligands (*HL1a* and *HL1b* for **4a** and **4b**, respectively) from the aldol reaction to the pyca aldehyde. In these structures, the ketone from the ligand *HL1a* or *HL1b* is now strongly bound to Cu ($\text{Cu(1)}-\text{O(1)}$ 2.038(3) Å), in contrast with previous neutral complexes derived from CuCl_2 (see, for instance, **1a–c** and **3a**) so that ligands *HL1a* and *HL1b* now act as tridentate chelating ligands $\kappa^3(\text{N},\text{O},\text{O}')$ as shown in Figure 7 for complexes **4a** and **4b**. Both structures are similar, having in both cases a distorted octahedral geometry around the Cu that arises from the coordination of two ligands in a tridentate fashion, reflecting the poor coordinating ability of ClO_4^- compared to Cl^- .

We noticed that the synthesis of **4a** led to very small amounts of additional species (as observed by ^1H NMR analysis of the reaction crude). After several tries to optimize the reaction conditions to study these new species, we found that the optimal conditions were to carry out the reaction in a CH_2Cl_2 /acetone mixture (see the Experimental Section). In this way, it was possible to isolate a small fraction of pale blue crystals of the binuclear complex **5** from the synthesis of complex **4a** (15% crystalline yield) (Figure 8a). The X-ray structure reveals that the dimer contains a novel anionic ligand (HLS^-) which results from the double aldol addition of pyca to one of the carbons of acetone

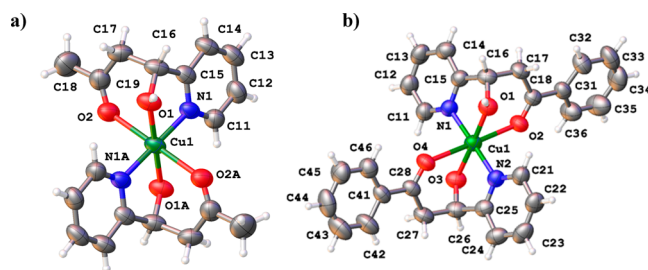


Figure 7. (a) Structure of the dication in **4a**, showing the atom numbering. The two ClO_4 anions have been omitted for clarity. Selected bond lengths (Å) and angles (deg): $\text{Cu(1)}-\text{N(1)}$ 1.945(4), $\text{Cu(1)}-\text{O(1)}$ 2.038(3), $\text{Cu(1)}-\text{O(2)}$ 2.283(4), $\text{O(1)}-\text{Cu(1)}-\text{N(1)}$ 82.18(2), $\text{O(2)}-\text{Cu(1)}-\text{N(1)}$ 86.47(2), $\text{O(1)}-\text{Cu(1)}-\text{O(2)}$ 79.54(2). (b) Structure of the dication in **4b**, showing the atom numbering. The two ClO_4 anions have been omitted for clarity. Selected bond lengths (Å) and angles (deg): $\text{Cu(1)}-\text{N(1)}$ 1.966(5), $\text{Cu(1)}-\text{O(1)}$ 1.904(4), $\text{Cu(1)}-\text{N(2A)}$ 1.978(5), $\text{Cu(1)}-\text{O(1A)}$ 1.948(4), $\text{Cu(1)}-\text{O(2A)}$ 2.336(4), $\text{Cu(1)}-\text{Cu(1A)}$ 2.948(2), $\text{N(1)}-\text{Cu(1)}-\text{N(2A)}$ 106.4(2), $\text{N(1)}-\text{Cu(1)}-\text{O(1)}$ 82.21(2), $\text{O(1)}-\text{Cu(1)}-\text{O(1A)}$ 80.14(2).

(see Figure 8b,c). Therefore, the dimer **5** is formed by two H_2LS ligands in which one of the OH groups of each ligand is deprotonated and the resulting alkoxo group bridges together two Cu atoms in a central Cu_2O_2 ring analogous to the one present in complex **3a** and similar to the structure of other dicopper complexes prepared in the literature by other means.²⁰ Although some cases of double aldol addition have been reported recently,²¹ these were conducted with an excess of a strong Lewis acid such as SiCl_4 or in strongly basic conditions. In these examples, the double addition product does not act as a ligand. The formation of **5**, however, proceeds at room temperature and in the absence of a base, and the novel HLS^- ligands act as pentadentate $\kappa^5(\text{N},\text{O},\text{O}',\text{O}'',\text{N}''')$ in which each pyridine arm coordinates a Cu atom. Importantly, ^1H NMR analysis of the reaction crude of several reactions showed that the second aldol reaction is regio- and stereoselective. Upon liberation of the H_2LS ligand, three species are observed, in a ratio of 47.5:47.5:5, all of which originate from the addition of two molecules of pyca to the same carbon of the acetone. That is, after the first aldol addition of pyca to acetone to give the simple aldol product, *HL1a*, the subsequent second aldol addition occurs via the attack of the methylene α -carbon protons to a second molecule of pyca. This implies that the reaction is regioselective and that the H_2LS ligand is produced exclusively as the double aldol product (i.e., there are no species resulting from the CH_3 enolate). The H_2LS ligand contains three chiral carbons (see Figure 8c), one of which is pseudoasymmetric, and could be present as a mixture of 4 stereoisomers: two meso compounds, RRS and RSS, and a pair of enantiomers, RR/SS (with coincident NMR signals); see the SI for details and notation. Out of these four stereoisomers, only the pair of enantiomers (RR/SS) and one of the meso forms are produced in significant proportions, while the formation of the other meso form is negligible (<5% of the double aldol product), thus giving rise to the two majority species observed by NMR (see the SI for further discussion and details). In other words, the double aldol addition of pyca to acetone promoted by $\text{Cu}(\text{ClO}_4)_2 \cdot 6\text{H}_2\text{O}$ is regio- and stereoselective. Although we do not know the exact details of this selectivity, we believe that coordination to copper plays a key role. Scheme 6 shows a tentative mechanism for the production of **5** and the observed stereoisomers. Initially, activation of pyca through coordination to Cu promotes the first aldol addition with acetone to produce a

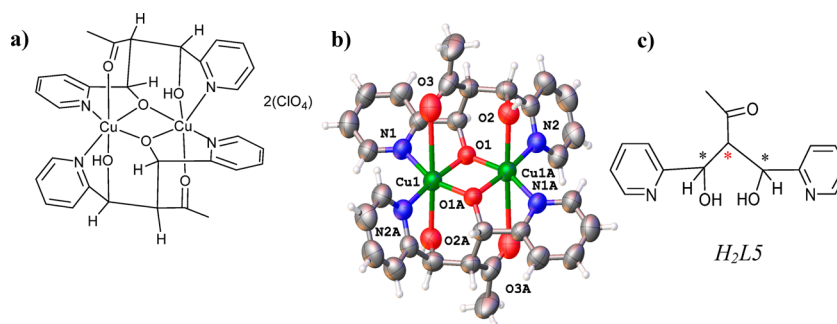
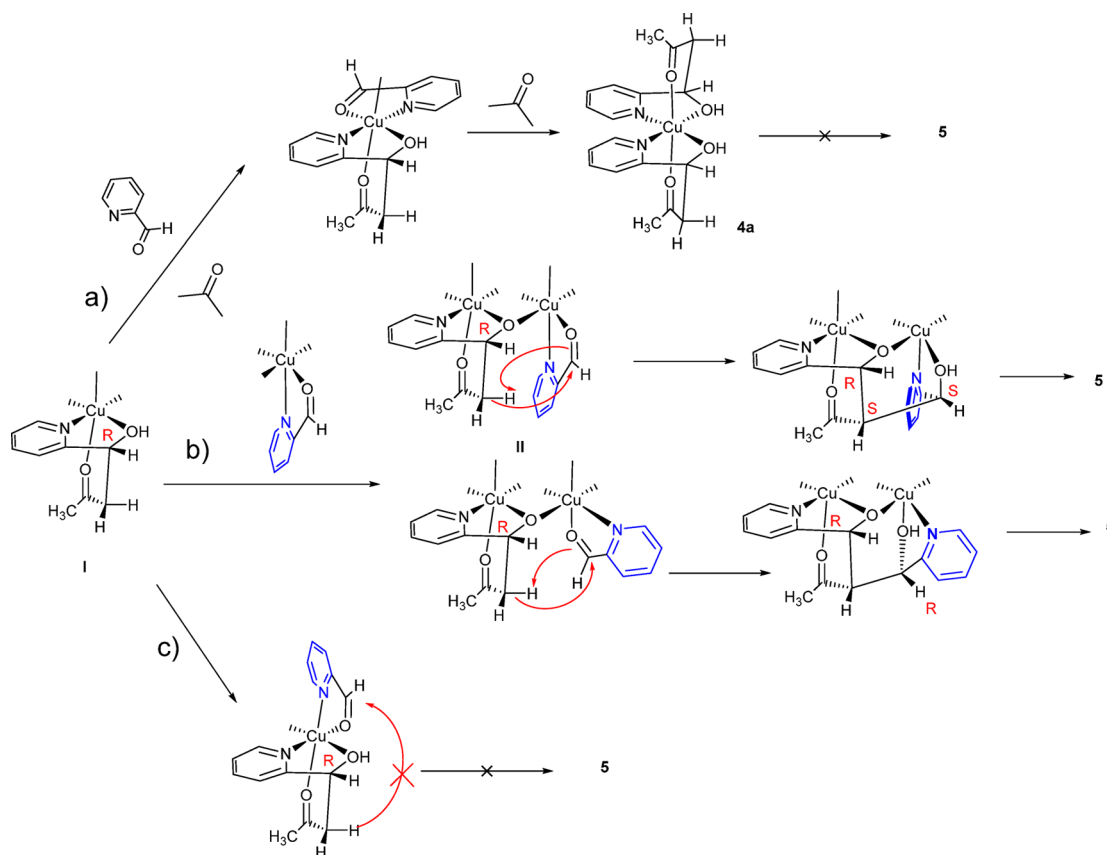


Figure 8. (a) Diagram of complex **5** showing that it consists of 2 anionic $HL5^-$ ligands. (b) X-ray structure of the dication **5**. The structure contains two ClO_4^- anions that have been omitted for clarity. Selected bond lengths (Å) and angles (deg): Cu(1)–N(1) 1.966(5), Cu(1)–O(1) 1.904(4), Cu(1)–N(2A) 1.978(5), Cu(1)–O(1A) 1.948(4), Cu(1)–O(2A) 2.336(4), N(1)–Cu(1)–N(2A) 106.4(2), N(1)–Cu(1)–O(1) 82.21(2), O(1)–Cu(1)–O(1A) 80.14(2). (c) H_2L5 ligand that results from the double addition of pyca to the same carbon of acetone. The ligand has three stereogenic centers; one of them, marked in red, is *pseudo asymmetric*. Note: Compound **5** is present as a mixture of stereoisomers. The X-ray diffraction structure shown in Figure 5b corresponds to only one of these stereoisomers. See Scheme 5 and later discussion.

Scheme 6. Tentative Mechanistic Pathway for the Stereo- and Regioselective Formation of 5, Involving a Double Aldol Addition of pyca to Acetone^a



^aThe reaction produces the novel H_2L5 ligand as a mixture of a pair of enantiomers (RR/SS) and the meso compound RSS, so two sets of signals are observed by NMR. For the sake of clarity, the diagram only shows the attack starting from the R- $HL1a$ ligand in intermediate **I** to give RR and the meso compound RSS. Attack from the other enantiomer, S- $HL1a$ (not shown) leads to the formation of SS and the meso compound SSR (same molecule as RSS). Note that the very small amount of the meso compound RRS (5%) observed by NMR could suggest that the coordination of the ketone in $HL1a$ in **I** is not strong enough to completely restrict the reaction of the enolate to one of the faces.

heteroleptic complex with an $HL1a$ ligand strongly coordinated in a tridentate fashion (compound **I** in Scheme 6). This complex could give the homoleptic complex **4a** via a second aldol reaction. However, the formation of **5** does not seem to involve the intermediacy of the homoleptic complex **4a** (see Scheme 6, path a), because reaction of **4a** with pyca and $Cu(ClO_4)_2 \cdot 6H_2O$ in the presence or absence of a base (K_2CO_3 or KOH) does not lead to

the formation of **5**. We also note that, due to geometric restraints, the intramolecular attack of pyca (i.e., from coordination of pyca to the same Cu complex instead of from a second Cu complex) is prevented (Scheme 6, path c). Therefore, the formation of **5** appears to involve an *intramolecular mechanism*. We propose that the reaction involves the initial formation of a dimer between compound **I** and another Cu-pyca complex to give complex **II**

(see Scheme 6, path b). The formation of such a complex is key because: (i) it brings together a second molecule of pyca activated by coordination of Cu; (ii) it restrains the reaction of the *HL1a* ligand to the closer CH₂ group (regioselectively) so that it would react with the pyca aldehyde though *only* one of the enolate faces (i.e., the face of the enolate pointing toward the O bridge rather than the one pointing to the *HL1a* pyridine). Although the enolate can react through only one of its faces (stereoselectively), it is able to attack both faces of the aldehyde (path b, above and below), yielding the two observed *H₂LS* species: a pair of enantiomers (RR/SS, with coincident NMR signals) and the meso compound RSS, but preventing the formation of the meso compound RRS. The formation of complex 5 would involve another sequence of reaction between a pyca molecule and a *HL1a* ligand to complete the formation of the dimeric complex shown in Figure 8. This is most straightforwardly realized from the intermolecular reaction between two heteroleptic Cu(*HLa*)(Pyca) complexes. Repeated attempts to produce double aldol addition of pyca to acetone under similar conditions using CuCl₂·2H₂O failed. This points out the critical role of the choice of the appropriate metal precursor with the right balance of Lewis acidity to produce a high enough degree of activation to the pyca aldehyde to undergo a second aldol addition to acetone while retaining regio- and stereoselectivity. The success of the reaction to obtain 5 therefore requires a metal complex precursor with enough Lewis acidity to promote a second aldol addition of pyca to acetone and with a nonsaturated coordination sphere so that formation of the O bridge can easily occur. The latter is also provided by weakly coordinated ClO₄[−] ligands, which also guarantee that the product of the first aldol addition, the *HL1a* ligand, is strongly coordinated in a tridentate fashion, thus defining the attacking face of the enolate. The very small amount of the other meso compound could suggest, however, that the ketone coordination of *HL1a* is not strong enough to induce complete stereoselectivity.

In principle, this reactivity could potentially be extended to other copper complexes that fulfill these requirements. In order to extend this reactivity to similar electron deficient complexes of copper, we also used Cu(BF₄)₂·6H₂O as a metal precursor instead of Cu(ClO₄)₂·6H₂O. We found that Cu(BF₄)₂ can also be used in this regio- and stereoselective double aldol reaction of acetone and pyca, producing 5·BF₄, the complex analogous to 5 with BF₄[−] anions instead of ClO₄[−]. The reaction proceeds with similar yields (15%; see the Experimental Section) and the complex 5·BF₄ could also be studied crystallographically (see the SI).

CONCLUSION

In conclusion, we found that the ability of copper to promote aldol addition can be used advantageously to develop procedures for the preparation of complexes in which the products of the aldol addition act as ligands in neutral complexes, when starting from CuCl₂·2H₂O, or cationic homoleptic complexes, when starting from Cu(ClO₄)₂·6H₂O. The copper atom in these reactions plays a 2-fold role: (i) the coordination of the oxygen of the ketone promotes the formation of the corresponding enolate, and (ii) the coordination of the oxygen of the aldehyde group of pyca enhances the electrophilic character of the aldehyde carbon, as shown by the calculations. The degree of activation of the pyca aldehyde depends on the choice of the metal precursor, thus opening a way to modulate its reactivity. More Lewis acidic Cu precursors such as Cu(ClO₄)₂ or Cu(BF₄)₂ result in a higher

degree of activation. In these cases, in addition to the formation of the simple aldol product, a small amount of double addition of pyca to acetone through a regio- and stereoselective reaction under mild and neutral conditions is also observed.

EXPERIMENTAL SECTION

Materials and General Methods. All reagents were purchased and used without further purification. Solvents were used as purchased. Kieselguhr (diatomaceous earth, Merck) was used for filtration. Column chromatography separations were carried out using silica gel 60 (particle size 0.040–0.063 mm; 230–400 mesh; Merck, Germany) as the stationary phase, and TLC was performed on precoated silica gel plates (0.25 mm thick, 60 F254, Merck, Germany) and observed under UV light. NMR spectra were recorded on Agilent DD2 500 instruments. ¹H and ¹³C NMR chemical shifts (δ) are reported in parts per million (ppm) and are referenced to TMS, using solvents as internal references. Coupling constants (*J*) are reported in hertz (Hz). Standard abbreviations are used to indicate multiplicity: s = singlet, d = doublet, t = triplet, m = multiplet. ¹H and ¹³C assignments were performed by utilizing 2D NMR methods (COSY, gradient CRISIS-HSQC, and gradient CRISIS-HMBC).²² Some quaternary carbon atoms were not detected, but they were located with the help of a ¹H–¹³C HMBC experiment. IR spectra of solid samples were recorded with a Frontier PerkinElmer Spectrum RX I FT-IR instrument. The magnetic moments were calculated from magnetic susceptibilities which were measured in Unidade de Magnetosusceptibilidade de Santiago de Compostela University. Elemental analyses were performed using a PerkinElmer 2400B microanalyzer. XRPD measurement (X-ray Powder Diffraction) was performed in the Laboratory of Instrumental Techniques of the University of Valladolid (L.T.I., www.laboratorioteccnicasinstrumentales.es) using a Bruker Discover D8. The XRPD patterns of all isolated compounds were coincident with those predicted by the software package MERCURY from the X-ray single crystal analysis (see the SI), thus confirming the identity of the bulk product. High resolution mass spectra were recorded at the mass spectrometry service of the Laboratory of Instrumental Techniques of the University of Valladolid as well. A MS-TOF (MS: Bruker Maxis Impact) by electrospray ionization (positive and negative ESI) was utilized. The HRMS spectra were analyzed using Bruker DataAnalysis 4.1 (www.bruker.com).

Synthesis of Complex 1a. To a green solution of CuCl₂·2H₂O (0.170 g, 1 mmol) in acetone (15 mL) was added pyridine-2-carboxaldehyde (pyca) (0.107 g, 1 mmol) with stirring. After 10 h, a green precipitate appeared. The solid was isolated by filtration with a fritted funnel. Yield 0.275 g, 92%. Anal. Calcd for C₉H₁₁Cl₂CuNO₂: C 36.06, H 3.70, N 4.67. Found C 36.23, H 3.63, N 4.17. μ_{eff} (293 K) 1.61 MB. A crystal suitable for X-ray determination was obtained by slow evaporation of a solution of CuCl₂·2H₂O with pyca in acetone.

Synthesis of Complex 1b. To a green solution of CuCl₂·2H₂O (0.170 g, 1 mmol) in THF (15 mL) were added pyridine-2-carboxaldehyde (pyca) (0.107 g, 1 mmol) and acetophenone in excess (0.600 g, 5 mmol) with stirring for 16 h. The resulting solution was concentrated, and hexane was added to obtain a green precipitate that was isolated by filtration and washed with hexane (3 × 10 mL). Yield 0.303 g, 84%. Anal. Calcd for C₁₄H₁₃Cl₂CuNO₂: C 46.49, H 3.62, N 3.87. Found C 46.35, H 3.63, N 3.92. μ_{eff} (293 K) 1.52 MB. A crystal suitable for X-ray determination was obtained by slow evaporation of a solution of CuCl₂·2H₂O (0.1 mmol) with pyca (0.1 mmol) in acetophenone (1 mL).

Synthesis of Complex 1c. To a green solution of CuCl₂·2H₂O (0.170 g, 1 mmol) in THF were added pyridine-2-carboxaldehyde (pyca) (0.107 g, 1 mmol) and 2-cyclohexen-1-one in excess (0.480 g, 5 mmol), and the solution was stirred for 16 h. After this time, an oil precipitate appeared. The crude was stirred with THF/ether 1:4 in an ultrasonic bath until a solid precipitate was obtained, which was isolated by filtration with a fritted funnel and dried under vacuum. Yield 0.290 g, 86%. Anal. Calcd for C₁₂H₁₃Cl₂CuNO: C 42.68, H 3.88, N 4.15. Found C 42.31, H 3.57, N 4.03. μ_{eff} (293 K) 1.46 MB. A crystal suitable for X-ray

determination was obtained by slow evaporation of a solution of $\text{CuCl}_2 \cdot 2\text{H}_2\text{O}$ (0.1 mmol) with pyca (0.1 mmol) in cyclohexanone (1 mL).

Synthesis of Complex 2. To a green solution of $\text{CuCl}_2 \cdot 2\text{H}_2\text{O}$ (0.170 g, 1 mmol) in methanol was added pyridine-2-carboxaldehyde (pyca) (0.321 g, 3 mmol) with stirring. After 15 min, a green precipitate appeared, and the solid was isolated by filtration with a fritted funnel. Yield 0.330 g, 92%. Anal. Calcd for $\text{C}_{12}\text{H}_{10}\text{Cl}_2\text{CuN}_2\text{O}_2$: C 41.34, H 2.89, N 8.03. Found C 41.28, H 2.75, N 8.17. IR ν (C=O) 1631 cm^{-1} . A crystal suitable for X-ray determination was obtained by slow evaporation of $\text{CuCl}_2 \cdot 2\text{H}_2\text{O}$ with pyca in methanol/ H_2O .

Synthesis of Complex 3a. To a green solution of **1a** (0.283 g, 1 mmol) in methanol was added sodium methoxide (0.054 g, 1 mmol) with stirring. After 15 min, a green precipitate appeared. The solid was collected in a frit, washed with water, and dried by suction. Yield 0.243 g, 92%. Anal. Calcd for $\text{C}_{18}\text{H}_{20}\text{Cl}_2\text{Cu}_2\text{N}_2\text{O}_4$: C 35.45, H 3.40, N 5.91. Found C 35.84, H 3.38, N 5.57. See magnetism data in the SI. A crystal suitable for X-ray determination was prepared as follows: Solid **1a** (0.150 g, 0.5 mmol) was dissolved in 5 mL of water in a vial (2 cm diameter, 10 cm height) and was covered with a layer of MeONa (0.5 mmol) in 5 mL of MeOH. The vial was left open to air. After several days of slow diffusion, a crop of suitable crystals had grown on the wall of the vial.

Synthesis of Complex 3b. Complex **3b** was prepared as described above for complex **3a** from a green solution of **1b** (0.360 g, 1 mmol) in methanol and MeONa (0.054 g, 1 mmol). Yield 0.304 g, 94%. Anal. Calcd for $\text{C}_{28}\text{H}_{24}\text{Cl}_2\text{Cu}_2\text{N}_2\text{O}_4$: C 51.70, H 3.72, N 4.31. Found C 51.73, H 3.91, N 4.45.

Synthesis of Complex 4a. To a light blue solution of $\text{Cu}(\text{ClO}_4)_2 \cdot 6\text{H}_2\text{O}$ (0.370 g, 1 mmol) in acetone was added pyridine-2-carboxaldehyde (pyca) (0.214 g, 2 mmol) with stirring. After 4 h, a green precipitate appeared, which was isolated by filtration with a fritted funnel. Yield 0.510 g, 86%. Anal. Calcd for $\text{C}_{18}\text{H}_{22}\text{CuCl}_2\text{N}_2\text{O}_{12}$: C 36.47, H 3.74, N 4.73. Found C 36.42, H 3.63, N 4.79. μ_{eff} (293 K) 1.51 MB. IR ν (C=O) 1692 cm^{-1} . A crystal suitable for X-ray determination was obtained by slow diffusion of $\text{Cu}(\text{ClO}_4)_2 \cdot 6\text{H}_2\text{O}$ and pyca in acetone. Note: No detectable amount of **5** was observed by following this procedure.

Synthesis of Complex 4b. To a light blue solution of $\text{Cu}(\text{ClO}_4)_2 \cdot 6\text{H}_2\text{O}$ (0.370 g, 1 mmol) in acetophenone was added pyridine-2-carboxaldehyde (pyca) (0.214 g, 2 mmol) with stirring. After 10 h, a green precipitate appeared, which was isolated by filtration with a fritted funnel. Yield 0.765 g, 91%. Anal. Calcd for $\text{C}_{28}\text{H}_{26}\text{CuCl}_2\text{N}_2\text{O}_{12}$: acetophenone: C 46.91 H 3.66, N 3.91. Found C 46.74, H 3.78, N 3.42. μ_{eff} (293 K) 1.01 MB. A crystal suitable for X-ray determination was obtained by slow evaporation of a solution of $\text{Cu}(\text{ClO}_4)_2 \cdot 6\text{H}_2\text{O}$ with pyca in acetophenone.

Synthesis of Complex 5. Slow crystallization at room temperature was required to obtain and isolate complex **5**. A layer consisting of a solution of $\text{Cu}(\text{ClO}_4)_2 \cdot 6\text{H}_2\text{O}$ (0.185 g, 0.5 mmol) in 10 mL of dichloromethane was deposited at the bottom of a vial (2 cm diameter, 10 cm height). A second layer of a solution of pyridine-2-carboxaldehyde (pyca) (0.107 g, 1 mmol) in acetone (10 mL) was carefully deposited on top. As the solvents diffused at room temperature over 48 h, light blue-green crystals of complex **5** appeared, which were dried under vacuum. Yield 0.032 g, 15%. Anal. Calcd for $\text{C}_{30}\text{H}_{30}\text{Cl}_2\text{Cu}_2\text{N}_4\text{O}_{14}$: C 41.49, H 3.48, N 6.45. Found C 41.22, H 3.15, N 6.17.

Note: Compound **5** is present as a mixture of stereoisomers.

Synthesis of Complex 5BF₄. Slow crystallization was required to obtain and isolate complex **5BF₄**. A layer consisting of a solution of $\text{Cu}(\text{BF}_4)_2 \cdot 6\text{H}_2\text{O}$ (0.173 g, 0.5 mmol) in 10 mL of dichloromethane was deposited at the bottom of a vial (2 cm diameter, 10 cm height). A second layer of a solution of pyridine-2-carboxaldehyde (pyca) (0.107 g, 1 mmol) in acetone (10 mL) was carefully deposited on top. As the solvents diffused, light blue-green crystals of complex **5BF₄** appeared. Yield 0.032 g, 15%. Anal. Calcd for $\text{C}_{30}\text{H}_{34}\text{B}_2\text{Cu}_2\text{F}_8\text{N}_4\text{O}_8$: C 40.98, H 3.90, N 6.37. Found C 40.78, H 3.78, N 6.81. Magnetism data are in the SI. IR ν (C=O) 1710 cm^{-1} .

General Procedure to Obtain Free Ligands HL1a–c and H₂L5. Typically, to a suspension of complexes **1a–c** (1 mmol) in dichloromethane (15 mL) was added NH_3 (25% aq) (3 \times 15 mL). After 10 min, the organic phase was extracted, dried with MgSO_4 , and

filtered through Kieselguhr. The resulting yellow-white oils/solids of the free ligands *HL1a–c* were evaporated to dryness, and the residues were dissolved in 1:1 AcOEt/hexane and filtered through silica gel. In the case of *H₂L5* liberation, the residue of the simple aldol addition was separated by chromatography using AcOEt/hexane mixtures. A 1:1 mixture was used to elute *HL1a* (the simple aldol product). Subsequently, a 3:1 mixture was used to elute *H₂L5*.

4-Hydroxy-4-(pyridin-2-yl)butan-2-one, (HL1a).²³ ¹H NMR (500 MHz, CDCl_3) δ 8.52 (ddd, J = 4.9, 1.8, 1.0 Hz, 1H, $\text{H}^{6\text{py}}$), 7.70 (td, J = 7.7, 1.8 Hz, 1H, $\text{H}^{4\text{py}}$), 7.45 (dq, J = 7.8, 1.0 Hz, 1H, $\text{H}^{3\text{py}}$), 7.20 (ddd, J = 7.5, 4.8, 1.1 Hz, 1H, $\text{H}^{5\text{py}}$), 5.19 (dd, J = 8.5, 3.6 Hz, 1H, H^{CH}), 4.19 (s, 1H, OH), 3.04 (dd, J = 17.1, 3.6 Hz, 1H, H^{CH_2}), 2.91 (dd, J = 17.1, 8.4 Hz, 1H, H^{CH_2}), 2.21 (s, 3H, CH_3). ¹³C NMR (126 MHz, CDCl_3): δ 207.45 C^{CO} , 161.51 $\text{C}^{2\text{py}}$, 148.14 $\text{C}^{6\text{py}}$, 136.57 $\text{C}^{4\text{py}}$, 122.23 $\text{C}^{5\text{py}}$, 120.35 $\text{C}^{3\text{py}}$, 69.54 C^{CH} , 50.60 C^{CH_2} , 30.73 C^{CH_3} ppm. Anal. Calcd for C 65.44, H 6.71, N 8.48. Found C 65.52, H 6.63, N 8.33. HR-MS (positive ion mode ESI-TOF): m/z for $\text{C}_9\text{H}_{11}\text{NNaO}_2$ [$M + \text{Na}$]⁺ calcd. 188.0682. Found 188.0687 (−2.7 pm error). IR ν (C=O) 1721 cm^{-1} .

3-Hydroxy-1-phenyl-3-(pyridin-2-yl)propan-1-one, (HL1b).²⁴ ¹H NMR (500 MHz, CDCl_3) δ 8.53 (ddd, J = 4.9, 1.8, 0.9 Hz, 1H, $\text{H}^{6\text{py}}$), 8.01–7.92 (m, 2H, $\text{H}^{2,6\text{Ph}}$), 7.70 (td, J = 7.7, 1.7 Hz, 1H, $\text{H}^{4\text{py}}$), 7.61–7.51 (m, 2H, $\text{H}^{4\text{Ph}}$ and $\text{H}^{3\text{py}}$), 7.44 (t, J = 7.8 Hz, 2H, $\text{H}^{3,5\text{Ph}}$), 7.19 (ddd, J = 7.5, 4.8, 1.1 Hz, 1H, $\text{H}^{5\text{py}}$), 5.39 (dd, J = 8.2, 3.6 Hz, 1H, H^{CH}), 4.36 (s, 1H, OH), 3.62 (dd, J = 17.4, 3.7 Hz, 1H, H^{CH_2}), 3.45 (dd, J = 17.4, 8.2 Hz, 1H, H^{CH_2}). ¹³C NMR (126 MHz, CDCl_3) δ 199.92 C^{CO} , 161.54 $\text{C}^{2\text{py}}$, 148.56 $\text{C}^{6\text{py}}$, 136.84 $\text{C}^{4\text{py}}$, 136.71 $\text{C}^{5\text{py}}$, 133.46 $\text{C}^{4\text{Ph}}$, 128.60 $\text{C}^{3,5\text{Ph}}$, 128.22 $\text{C}^{2,6\text{Ph}}$, 122.41 $\text{H}^{5\text{py}}$, 120.49 $\text{H}^{3\text{py}}$, 70.19 C^{CH} , 45.97 C^{CH_2} ppm. Anal. Calcd for C 73.99, H 5.77, N 6.16. Found C 73.75, H 5.59, N 6.06. HR-MS (positive ion mode ESI-TOF): m/z for $\text{C}_{14}\text{H}_{13}\text{NNaO}_2$ [$M + \text{Na}$]⁺ calcd. 250.0838. Found 250.0840 (−0.6 pm error).

(S)-6-((R)-6-(Hydroxy(pyridin-2-yl)methyl)cyclohex-2-en-1-one and (R)-6-((R)-Hydroxy(pyridin-2-yl)methyl)cyclohex-2-en-1-one, (HL1c). ¹H NMR (500 MHz, CDCl_3) δ 8.55 (ddd, J = 4.9, 1.8, 1.0 Hz, 1H, $\text{H}^{6\text{py,anti}}$), 7.68 (td, J = 7.7, 1.7 Hz, 1H, $\text{H}^{4\text{py,anti}}$), 7.41 (dt, J = 8.0, 1.1 Hz, 1H, $\text{H}^{3\text{py,anti}}$), 7.21 (ddd, J = 7.5, 4.9, 1.3 Hz, 1H, $\text{H}^{5\text{py,anti}}$), 6.97 (dt, J = 9.8, 4.1, 1H, $\text{H}^{3(\text{CH}=\text{CH})\text{anti}}$), 6.10 (dd, J = 10.0, 2.8 Hz, $\text{H}^{2(\text{CH}=\text{CH})\text{syn}}$), 6.03 (dt, J = 10.0, 2.0 Hz, 1H, $\text{H}^{2(\text{CH}=\text{CH})\text{anti}}$), 5.60 (d, J = 2.93 Hz, 1H, $\text{H}^7(\text{CH}=\text{CH})\text{syn}$), 5.20 (d, J = 5.9 Hz, 1H, $\text{H}^7(\text{CH}=\text{CH})\text{anti}$), 2.96 (ddd, J = 13.4, 6.0, 4.7 Hz, 1H, $\text{H}^{6\text{anti}}$), 2.87 (ddd, J = 13.2, 4.7, 2.9 Hz, 1H, $\text{H}^{6\text{syn}}$), 2.35 (dtd, J = 8.0, 4.2, 2.2 Hz, 2H, $\text{H}^{4\text{anti}}$), 1.89–1.79 (m, 1H, $\text{H}^{5\text{b anti}}$), 1.63–1.50 (m, 1H, $\text{H}^{5\text{a anti}}$). ¹³C NMR (126 MHz, CDCl_3) δ 202.89 $\text{C}^{\text{CO,anti}}$, 160.30 $\text{C}^{2\text{py,anti}}$, 151.16 $\text{C}^{3(\text{C}=\text{C})\text{anti}}$, 148.22 $\text{C}^{6\text{py,anti}}$, 136.80, $\text{C}^{4\text{py,anti}}$, 130.01 $\text{C}^{2(\text{C}=\text{C})\text{syn}}$, 129.83 $\text{C}^{2(\text{C}=\text{C})\text{anti}}$, 122.58 $\text{C}^{5\text{py,anti}}$, 121.72 $\text{C}^{3\text{py,anti}}$, 73.52 $\text{C}^{7\text{anti}}$, 70.70 $\text{C}^{7\text{syn}}$, 52.75 $\text{C}^{6\text{anti}}$, 48.72 $\text{C}^{6\text{syn}}$, 25.82 C^{anti} , 24.60 C^{santi} ppm. Anal. Calcd for C 70.92, H 6.45, N 6.89. Found C 70.79, H 6.38, N 6.93. HR-MS (positive ion mode ESI-TOF): m/z for $\text{C}_{12}\text{H}_{13}\text{NNaO}_2$ [$M + \text{Na}$]⁺ calcd. 226.0838. Found 226.0844 (−2.6 pm error).

Note: SR is the syn isomer and RR is the anti isomer of the aldol addition.

4-Hydroxy-3-(hydroxy(pyridin-2-yl)methyl)-4-(pyridin-2-yl)butan-2-one, (H₂L5). ¹H NMR (500 MHz, CDCl_3) δ 8.55 (ddd, J = 9.5, 4.9, 1.8, 2H, $\text{H}^{6\text{py,RR/SS}}$), 8.49 (ddd, J = 4.9, 1.8, 0.9 Hz, 2H, $\text{H}^{6\text{py,RSS}}$), 7.70 (td, J = 7.7, 1.6, 2H, $\text{H}^{4\text{py,RR/SS}}$), 7.66 (td, J = 7.8, 1.7, 2H, $\text{H}^{4\text{py,RSS}}$), 7.54–7.48 (m, 2H, $\text{H}^{3\text{py,RR/SS}}$), 7.45 (dd, J = 7.8, 0.9 Hz, 2H, $\text{H}^{3\text{py,RSS}}$), 7.21 (ddd, J = 7.6, 4.8, 1.2 Hz, 2H, $\text{H}^{5\text{py,RR/SS}}$), 7.15 (ddd, J = 7.7, 4.8, 1.1 Hz, 2H, $\text{H}^{5\text{py,RSS}}$), 5.37 (d, J = 5.8 Hz, 1H, $\text{CHOH}^{\text{RR/SS}}$), 5.12 (d, J = 2.8 Hz, 1H, $\text{CHOH}^{\text{RR/SS}}$), 5.01 (d, J = 5.8 Hz, 2H, CHOH^{RSS}), 3.99 (dd, J = 5.9, 2.8 Hz, 1H, $\text{CHCO}^{\text{RR/SS}}$), 3.75 (t, J = 5.8 Hz, 1H, CHCO^{RSS}), 1.99 (s, 3H, CH_3^{RSS}), 1.81 (s, 3H, $\text{CH}_3^{\text{RR/SS}}$). ¹³C NMR (126 MHz, CDCl_3) δ 213.6 $\text{C}^{\text{CO,RSS}}$, 211.2 $\text{C}^{\text{CO,RR}}$, 160.4 $\text{C}^{2\text{py,RR/SS}}$, 160.4 $\text{C}^{2\text{py,RSS}}$, 148.65 $\text{C}^{6\text{py,RR/SS}}$, 148.23 $\text{C}^{6\text{py,RSS}}$, 136.71 $\text{C}^{4\text{py,RR/SS}}$, 136.59 $\text{C}^{4\text{py,RSS}}$, 122.59 $\text{C}^{5\text{py,RR/SS}}$, 122.21 $\text{C}^{5\text{py,RSS}}$, 121.11 $\text{C}^{3\text{py,RR/SS}}$, 120.69 $\text{C}^{3\text{py,RSS}}$, 73.50 $\text{C}^{\text{CHOH,RSS}}$, 73.05 $\text{C}^{\text{CHOH,RR/SS}}$, 72.08 $\text{C}^{\text{CHCO,RR/SS}}$, 61.81 $\text{C}^{\text{CHCO,RSS}}$, 61.75 $\text{C}^{\text{CHCO,RR/SS}}$, 33.58 $\text{C}^{\text{CH}_3,\text{RSS}}$, 31.60 $\text{C}^{\text{CH}_3,\text{RR/SS}}$ ppm. HR-MS (positive ion mode ESI-TOF): m/z for $\text{C}_{15}\text{H}_{17}\text{N}_2\text{O}_3$ [$M + \text{H}$]⁺ calcd 273.1234. Found 273.1235 (−0.7 pm error).

Note: A small amount (typically $\leq 5\%$) of the meso form SRR is also present. δ 8.46 (m, 1H, $\text{H}^{6\text{py}}$), 5.22 (d, J = 5.5 Hz, 2H, CHOH), 3.90 (t, J

Table 1. Crystal Data, Particular Details, and CCDC Reference Numbers

	1a	1b	1c	2
formula	C ₁₈ H ₂₂ Cl ₄ Cu ₂ N ₂ O ₄	C ₁₄ H ₁₃ Cl ₂ CuNO ₂	C ₂₈ H ₃₄ Cl ₄ Cu ₂ N ₂ O ₅	C ₁₂ H ₁₀ Cl ₂ CuN ₂ O ₂
<i>M</i> _f	599.25	361.69	747.45	348.66
crystal system	triclinic	orthorhombic	monoclinic	monoclinic
space group	<i>P</i> $\bar{1}$	<i>Pbca</i>	<i>P</i> ₂ ₁ / <i>c</i>	<i>P</i> ₂ ₁ / <i>c</i>
<i>a</i> [Å]	8.5131(8)	7.8681(5)	19.0706(5)	7.2339(7)
<i>b</i> [Å]	8.6879(8)	17.6088(18)	11.9615(3)	8.4932(11)
<i>c</i> [Å]	9.1287(7)	20.976(3)	14.8605(4)	11.2227(10)
α [deg]	93.824(7)	90	90	90.00
β [deg]	114.005(9)	90	107.578(3)	94.101(9)
γ [deg]	105.792(9)	90	90	90.00
<i>V</i> [Å ³]	581.28(10)	2906.1(5)	3231.57(16)	687.75(13)
<i>Z</i>	1	8	4	2
ρ [Mg m ^{−3}]	1.712	1.653	1.536	1.684
μ (Mo <i>K</i> α) [mm ^{−1}]	2.316	1.869	1.685	1.973
crystal size [mm]	0.2084 × 0.1521 × 0.1131	0.29 × 0.0827 × 0.0605	0.3484 × 0.136 × 0.1154	0.295 × 0.128 × 0.094
<i>F</i> (000)	302.0	1464.0	1528.0	350.0
θ range [deg]	4.974–57.186	4.626–57.162	4.076–57.218	5.64–57.56
refl. collected	3724	7468	13 830	2743
indep. refl. [<i>R</i> (int)]	2577 [0.0309]	3294 [0.0814]	7192 [0.0258]	1547 [0.0324]
GOF on <i>F</i> ²	1.086	1.036	1.033	0.895
data/restraints/parameters	2577/0/137	3294/0/181	7192/0/370	89/0
<i>R</i> ₁ (on <i>F</i> , <i>I</i> > 2 σ (<i>I</i>))	0.0583	0.0794	0.0479	0.0574
<i>wR</i> ₂ (on <i>F</i> ² , all data)	0.1081	0.1774	0.1195	0.1693
max/min $\Delta\rho$ [e Å ^{−3}]	0.67/−0.36	0.53/−0.47	0.61/−0.44	1.27/−0.54
CCDC number	1576053	1576054	1576055	1491834
	3a	4a	4b	5
formula	C ₃₆ H ₄₀ Cl ₄ Cu ₄ N ₄ O ₈	C ₁₈ H ₂₂ Cl ₂ CuN ₂ O ₁₂	C ₃₆ H ₃₄ Cl ₂ CuN ₂ O ₁₃	C ₃₆ H ₄₆ Cl ₂ Cu ₂ N ₄ O ₁₈
<i>M</i> _f	1052.68	592.81	837.09	1020.75
crystal system	orthorhombic	triclinic	monoclinic	triclinic
space group	<i>Fddd</i>	<i>P</i> $\bar{1}$	<i>P</i> ₂ ₁ / <i>n</i>	<i>P</i> $\bar{1}$
<i>a</i> [Å]	14.5777(7)	7.8646(5)	12.9342(3)	7.5652(7)
<i>b</i> [Å]	21.1806(8)	8.5460(8)	10.6919(3)	11.0310(11)
<i>c</i> [Å]	29.7098(12)	9.4424(8)	26.9101(7)	14.7049(14)
α [deg]	90	75.641(7)	90	104.540(9)
β [deg]	90	79.517(6)	94.257(2)	103.136(9)
γ [deg]	90	76.302(7)	90	103.882(8)
<i>V</i> [Å ³]	9173.3(7)	592.18(9)	3711.16(15)	1097.9(2)
<i>Z</i>	8	1	4	1
ρ [Mg m ^{−3}]	1.524	1.662	1.498	1.544
μ (Mo <i>K</i> α) [mm ^{−1}]	2.111	1.213	0.801	2.992
crystal size [mm]	0.387 × 0.246 × 0.147	0.2631 × 0.1911 × 0.1005	0.4313 × 0.3083 × 0.2226	0.1552 × 0.0704 × 0.0552
<i>F</i> (000)	4256.0	303.0	1724.0	526.0
θ range [deg]	5.332–59.024	4.492–57.176	4.1–59.688	6.522–143.61
refl. collected	7783	3773	20 894	6996
indep. refl. [<i>R</i> (int)]	2775 [0.0366]	2655 [0.0227]	8957 [0.0255]	4168 [0.0556]
GOF on <i>F</i> ²	1.076	1.050	1.045	0.977
data/restraints/parameters	2775/0/128	2655/68/189	8957/136/544	4168/68/314
<i>R</i> ₁ (on <i>F</i> , <i>I</i> > 2 σ (<i>I</i>))	0.0384	0.0614	0.0624	0.0739
<i>wR</i> ₂ (on <i>F</i> ² , all data)	0.0991	0.1717	0.2078	0.2413
max/min $\Delta\rho$ [e Å ^{−3}]	0.45/−0.47	0.50/−0.34	0.70/−0.59	0.55/−0.70
CCDC number	1576056	1576057	1576058	1576059

= 5.4 Hz, 1H, CHCO), 2.14 (s, 3H, CH₃) ppm. The rest of the signals overlapped with the signals of the other two major isomers.

Computational Details. All calculations were performed using the Gaussian 09 software package,²⁵ using the PBE1PBE method. This hybrid Hartree–Fock/density functional model is based on the Perdew–Burke–Ernzerhof (PBE) functional, where the HF/DFT exchange ratio is fixed *a priori* to 1:4, and was used to optimize the ground state geometries. Geometry optimizations were performed without symmetry restrictions, using initial coordinates derived from X-

ray data of the same compounds when available, and frequency analyses were performed to ensure that a minimum structure with no imaginary frequencies was achieved in each case. On the basis of the optimized ground geometries, a Natural Bond Order (NBO) analysis was performed at the PBE1PBE level associated with the PCM method (in acetone) to introduce the solvent effects.²⁶ In the calculations, effective core potentials (ECP) and their associated SDD basis set were used for the copper atoms,²⁷ while the light elements (Cl, O, N, C, and H) were described with the cc-pVTZ basis.²⁸ The graphical

representations of the compounds in their ground state geometries were made using GaussView.²⁹

X-ray Diffraction Study of 1a–c, 2, 3a–b, 4a–b, 5. Diffraction data were collected using an Oxford Diffraction Supernova diffractometer, equipped with an Atlas CCD area detector and a four-circle kappa goniometer. For the data collection, Mo or Cu microfocus sources with multilayer optics were used. Data integration, scaling, and empirical absorption correction were carried out using the CrysAlis Pro software package.³⁰ The structure was solved using direct methods and refined by Full-Matrix-Least-Squares against F^2 with SHELX³¹ under OLEX2.³² The non-hydrogen atoms were refined anisotropically, and hydrogen atoms were placed at idealized positions and refined using the riding model. Graphics were made with OLEX2 and MERCURY.³³ Crystal data, particular details, and CCDC reference numbers are given in Table 1.

■ ASSOCIATED CONTENT

■ Supporting Information

The Supporting Information is available free of charge on the ACS Publications website at DOI: 10.1021/acs.inorgchem.7b02448.

Crystallographic data, comparison of XRPD patterns of the bulk samples and the patterns predicted by XRD single crystal analysis, graphs of χ^2 vs T for complexes 3a and 5, HRMS spectrum of ligand H_2L5 , and 1H NMR spectra of free ligands $HL1a$ – c and H_2L5 (PDF)

Accession Codes

CCDC 1491834 and 1576053–1576061 contain the supplementary crystallographic data for this paper. These data can be obtained free of charge via www.ccdc.cam.ac.uk/data_request/cif, or by emailing data_request@ccdc.cam.ac.uk, or by contacting The Cambridge Crystallographic Data Centre, 12 Union Road, Cambridge CB2 1EZ, UK; fax: +44 1223 336033.

■ AUTHOR INFORMATION

Corresponding Authors

*E-mail: dmsj@qi.uva.es (D.M.).

*E-mail: raul.garcia.rodriquez@uva.es (R.G.-R.).

ORCID

José M. Martín Álvarez: 0000-0002-6969-0703

Raúl García-Rodríguez: 0000-0003-0699-3894

Daniel Miguel: 0000-0003-0650-3058

Author Contributions

The manuscript was written through contributions of all authors.

Notes

The authors declare no competing financial interest.

■ ACKNOWLEDGMENTS

This research was supported by the Spanish Ministerio de Economía y Competitividad (MINECO) (project number CTQ 2013-41067-P). R.G.-R. acknowledges the Spanish MINECO-AEI and the European Union (ESF) for a Ramon y Cajal contract (RYC-2015–19035).

■ REFERENCES

- (1) (a) Zweifel, G. S.; Nantz, M. H.; Somfai, P. Organocopper Reagents. In *Modern Organic Synthesis: An Introduction*, 2nd ed.; W. H. Freeman: New York, 2017.
- (2) For selected recent examples, see: (a) Weidner, K.; Sun, Z.; Kumagai, N.; Shibasaki, M. Direct Catalytic Asymmetric Aldol Reaction of an α -Azido Amide. *Angew. Chem., Int. Ed.* **2015**, *54*, 6236–6240. (b) Li, Z.; Li, R.; Gan, M.; Jiang, L.; Li, Z. Copper-catalyzed domino reactions: conjugate alkylative aldol addition/lactonization of α,β -

- unsaturated diesters. *Tetrahedron Lett.* **2015**, *56*, 5541–5544. (c) Shi, S.; Wei, X.; Shimizu, Y.; Kanai, M. Copper(I)-Catalyzed Enantioselective Incorporation of Ketones to Cyclic Hemiaminals for the Synthesis of Versatile Alkaloid Precursors. *J. Am. Chem. Soc.* **2012**, *134*, 17019–17022. (d) Bhimireddy, E.; Corey, E. J. Method for Highly Enantioselective Ligation of Two Chiral C(sp³) Stereocenters. *J. Am. Chem. Soc.* **2017**, *139*, 11044–11047. (e) Noda, H.; Amemiya, F.; Weidner, K.; Kumagai, N.; Shibasaki, M. Catalytic asymmetric synthesis of CF₃-substituted tertiary propargylic alcohols via direct aldol reaction of [small alpha]-N3 amide. *Chem. Sci.* **2017**, *8*, 3260–3269.

(3) Mahrwald, R. *Modern Aldol Reactions*; Wiley-VCH Verlag: Weinheim, Germany, 2008.

(4) See, for instance, the following reviews: (a) Mohr, J. T.; Krout, M. R.; Stoltz, B. M. Natural products as inspiration for the development of asymmetric catalysis. *Nature* **2008**, *455*, 323–332. (b) Dondoni, A.; Massi, A. Asymmetric Organocatalysis: From Infancy to Adolescence. *Angew. Chem., Int. Ed.* **2008**, *47*, 4638–4660.

(5) (a) Trost, B. M.; Brindle, C. S. The direct catalytic asymmetric aldol reaction. *Chem. Soc. Rev.* **2010**, *39*, 1600–1632. (b) Matsuo, J.-i.; Murakami, M. The Mukaiyama Aldol Reaction: 40 Years of Continuous Development. *Angew. Chem., Int. Ed.* **2013**, *52*, 9109–9118.

(6) Gati, W.; Yamamoto, H. Second Generation of Aldol Reaction. *Acc. Chem. Res.* **2016**, *49*, 1757–1768. (b) Cowden, C. J.; Paterson, I. Asymmetric Aldol Reactions Using Boron Enolates. In *Organic Reactions*; John Wiley & Sons: Hoboken, NJ, 2004.

(7) (a) Mlynarski, J.; Bas, S. Catalytic asymmetric aldol reactions in aqueous media - a 5 year update. *Chem. Soc. Rev.* **2014**, *43*, 577–587. (b) Mlynarski, J.; Paradowska, J. Catalytic asymmetric aldol reactions in aqueous media. *Chem. Soc. Rev.* **2008**, *37*, 1502–1511.

(8) (a) Evans, D. A.; Kozlowski, M. C.; Murry, J. A.; Burgey, C. S.; Campos, K. R.; Connell, B. T.; Staples, R. J. C2-Symmetric Copper(II) Complexes as Chiral Lewis Acids. Catalytic Enantioselective Aldol Additions of Silylketene Acetals to (Benzyloxy)acetaldehyde. *J. Am. Chem. Soc.* **1999**, *121*, 669–685. (b) Evans, D. A.; Fitch, D. M.; Smith, T. E.; Cee, V. J. Application of Complex Aldol Reactions to the Total Synthesis of Phorboxazole B. *J. Am. Chem. Soc.* **2000**, *122*, 10033–10046.

(9) Johnson, J. S.; Nicewicz, D. A. Copper Lewis Acids. In *Modern Aldol Reactions*; Wiley-VCH Verlag: Weinheim, Germany, 2008; pp 69–103.

(10) (a) Lalic, G.; Aloise, A. D.; Shair, M. D. An Exceptionally Mild Catalytic Thioester Aldol Reaction Inspired by Polyketide Biosynthesis. *J. Am. Chem. Soc.* **2003**, *125*, 2852–2853. (b) Serra-Pont, A.; Alfonso, I.; Sola, J.; Jimeno, C. A copper-templated, bifunctional organocatalyst: a strongly cooperative dynamic system for the aldol reaction. *Org. Biomol. Chem.* **2017**, *15*, 6584–6591. (c) Iwata, M.; Yazaki, R.; Chen, I. H.; Sureshkumar, D.; Kumagai, N.; Shibasaki, M. Direct Catalytic Enantio- and Diastereoselective Aldol Reaction of Thioamides. *J. Am. Chem. Soc.* **2011**, *133*, 5554–5560. (d) Bao, Y.; Kumagai, N.; Shibasaki, M. Managing the retro-pathway in direct catalytic asymmetric aldol reactions of thioamides. *Chem. Sci.* **2015**, *6*, 6124–6132. (e) Xu, Z.; Daka, P.; Wang, H. Primary amine-metal Lewis acid bifunctional catalysts: the application to asymmetric direct aldol reactions. *Chem. Commun.* **2009**, 6825–6827. (f) Daka, P.; Xu, Z.; Alexa, A.; Wang, H. Primary amine-metal Lewis acid bifunctional catalysts based on a simple bidentate ligand: direct asymmetric aldol reaction. *Chem. Commun.* **2011**, *47*, 224–226.

(11) Hazra, S.; Karmakar, A.; Guedes da Silva, M. d. F. C.; Dhan, L.; Boca, R.; Pombeiro, A. J. L. Sulfonated Schiff base dinuclear and polymeric copper(II) complexes: crystal structures, magnetic properties and catalytic application in Henry reaction. *New J. Chem.* **2015**, *39*, 3424.

(12) (a) Szpakolski, K. B.; Latham, K.; Rix, C. J.; White, J. M. Di(2-pyridyl) Ketone Complexes of Cu^I- and Cu^{II}-Containing Iodide and Thiocyanate Ligands: An Unusual Case of a Mixed-Aldol Condensation. *Eur. J. Inorg. Chem.* **2010**, *2010*, 5660–5667. (b) Deschamps, P.; Kulkarni, P. P.; Sarkar, B. The Crystal Structure of a Novel Copper(II) Complex with Asymmetric Ligand Derived from L-Histidine. *Inorg. Chem.* **2003**, *42*, 7366–7368.

(13) Kitos, A. A.; Efthymiou, C. G.; Manos, M. J.; Tasiopoulos, A. J.; Nastopoulos, V.; Escuer, A.; Perlepes, S. P. Interesting copper(II)-

assisted transformations of 2-acetylpyridine and 2-benzoylpyridine. *Dalton Trans.* **2016**, 45, 1063–1077.

(14) Álvarez, C. M.; García-Rodríguez, R.; Miguel, D. Iminopyridine Complexes of Manganese, Rhenium, and Molybdenum Derived from Amino Ester Methylserine and Peptides Gly-Gly, Gly-Val, and Gly-Gly-Gly: Self-Assembly of the Peptide Chains. *Inorg. Chem.* **2012**, 51, 2984–2996. (b) Álvarez, C. M.; García-Rodríguez, R.; Martín-Álvarez, J. M.; Miguel, D. Unexpected chemoselectivity in the Schiff condensation of amines with η^2 (C,O)- η^1 (O)-coordinated aldehyde. *Dalton Trans.* **2010**, 39, 1201–1203. (c) Álvarez, C. M.; García-Rodríguez, R.; Miguel, D. Pyridine-2-carboxaldehyde as ligand: Synthesis and derivatization of carbonyl complexes. *Dalton Trans.* **2007**, 3546–3554. (d) Álvarez, C. M.; García-Rodríguez, R.; Miguel, D. Carbonyl complexes of manganese, rhenium and molybdenum with 2-pyridylimino acid ligands. *J. Organomet. Chem.* **2007**, 692, 5717–5726.

(15) (a) Alvarez, C. M.; Carrillo, R.; Garcia-Rodriguez, R.; Miguel, D. pH-driven dynamic stereoselection: epimerization upon dimerization in rhenium(I) complexes. *Chem. Commun.* **2011**, 47, 12765–12767. (b) Alvarez, C. M.; Carrillo, R.; Garcia-Rodriguez, R.; Miguel, D. Stereoselective Aldol Addition to Rhenium(I) Complexes and Reversible Dimerization with Epimerization of the Metal Center. *Chem. - Eur. J.* **2013**, 19, 8285–8293.

(16) (a) Machajewski, T. D.; Wong, C.-H. The Catalytic Asymmetric Aldol Reaction. *Angew. Chem., Int. Ed.* **2000**, 39, 1352–1374. (b) Darbre, T.; Machuqueiro, M. Zn-Proline catalyzed direct aldol reaction in aqueous media. *Chem. Commun.* **2003**, 1090–1091. (c) Kofoed, J.; Darbre, T.; Reymond, J.-L. Dual mechanism of zinc-proline catalyzed aldol reactions in water. *Chem. Commun.* **2006**, 1482–1484.

(17) (a) Zhong, Z.; Postnikova, B. J.; Hanes, R. E.; Lynch, V. M.; Anslyn, E. V. Large pKa Shifts of α -Carbon Acids Induced by Copper(II) Complexes. *Chem. - Eur. J.* **2005**, 11, 2385–2394. (b) Fessner, W.-D.; Schneider, A.; Held, H.; Sinerius, G.; Walter, C.; Hixon, M.; Schloss, J. V. The Mechanism of Class II, Metal-Dependent Aldolases. *Angew. Chem., Int. Ed. Engl.* **1996**, 35, 2219–2221.

(18) Addison, A. W.; Rao, T. N.; Reedijk, J.; Van Rijn, J.; Verschoor, G. C. Synthesis, structure, and spectroscopic properties of copper(II) compounds containing nitrogen-sulphur donor ligands; the crystal and molecular structure of aqua[1,7-bis(N-methylbenzimidazol-2[prime or minute]-yl)-2,6-dithiaheptane]copper(II) perchlorate. *J. Chem. Soc., Dalton Trans.* **1984**, 1349.

(19) Crassous, J. Chiral transfer in coordination complexes: towards molecular materials. *Chem. Soc. Rev.* **2009**, 38, 830–845.

(20) Drew, M. G. B.; Naskar, J. P.; Chowdhury, S.; Datta, D. A Fluxional $\text{Cu}^{\text{I}}\text{N}_2\text{O}_2$ Core: Binding of a Keto Oxygen Atom to Cu^{I} and Ag^{I} . *Eur. J. Inorg. Chem.* **2005**, 2005, 4834–4839.

(21) (a) Abiko, A. Boron-Mediated Aldol Reaction of Carboxylic Esters. *Acc. Chem. Res.* **2004**, 37, 387–395. (b) Abiko, A.; Inoue, T.; Furuno, H.; Schwalbe, H.; Fieres, C.; Masamune, S. The First Doubly Borylated Enolate as an Intermediate of the Double Aldol Reaction. *J. Am. Chem. Soc.* **2001**, 123, 4605–4606. (c) Abiko, A.; Inoue, T.; Masamune, S. Mechanism of the Double Aldol Reaction: The First Spectroscopic Characterization of a Carbon-Bound Boron Enolate Derived from Carboxylic Esters. *J. Am. Chem. Soc.* **2002**, 124, 10759–10764. (d) Maier, F.; Trapp, O. Selector-Induced Dynamic Deracemization of a Selectand-Modified Tropos BIPHEPO-Ligand: Application in the Organocatalyzed Asymmetric Double-Aldol-Reaction. *Angew. Chem., Int. Ed.* **2014**, 53, 8756–8760. (e) Shimoda, Y.; Kotani, S.; Sugiura, M.; Nakajima, M. Enantioselective Double Aldol Reaction Catalyzed by Chiral Phosphine Oxide. *Chem. - Eur. J.* **2011**, 17, 7992–7995.

(22) (a) Kaerner, A.; Rabenstein, D. L. An ω_1 -band-selective, ω_1 -homonuclear decoupled ROESY experiment: application to the assignment of ^1H NMR spectra of difficult-to-assign peptide sequences. *Magn. Reson. Chem.* **1998**, 36, 601–607. (b) Gaillet, C.; Lequart, C.; Debeire, P.; Nuzillard, J.-M. Band-Selective HSQC and HMBC Experiments Using Excitation Sculpting and PFGSE. *J. Magn. Reson.* **1999**, 139, 454–459. (c) Crouch, R.; Boyer, R. D.; Johnson, R.; Krishnamurthy, K. Broadband and band-selective IMPRESS-gHMBC: compensation of refocusing inefficiency with synchronized inversion

sweep. *Magn. Reson. Chem.* **2004**, 42, 301–307. (d) Hu, H.; Krishnamurthy, K. Doubly compensated multiplicity-edited HSQC experiments utilizing broadband inversion pulses. *Magn. Reson. Chem.* **2008**, 46, 683–689.

(23) (a) Chimni, S. S.; Mahajan, D. Electron deficiency of aldehydes controls the pyrrolidine catalyzed direct cross-aldol reaction of aromatic/heterocyclic aldehydes and ketones in water. *Tetrahedron* **2005**, 61 (21), 5019–5025. (b) Marvel, C. S.; Stille, J. K. Preparation of the pyridalacetones and the inductive effect of nitrogen on the degradation of the intermediate aldols. *J. Org. Chem.* **1957**, 22, 1451–1457.

(24) Loh, T.-P.; Liung, S. B. K. W.; Tan, K.-L.; Wei, L.-L. Three Component Synthesis of β -Amino Carbonyl Compounds Using Indium Trichloride-Catalyzed One-pot Mannich-type Reaction in Water. *Tetrahedron* **2000**, 56, 3227–3237.

(25) Frisch, M. J.; Trucks, G. W.; Schlegel, H. B.; Scuseria, G. E.; Robb, M. A.; Cheeseman, J. R.; Scalmani, G.; Barone, V.; Mennucci, B.; Petersson, G. A.; Nakatsuji, H.; Caricato, M.; Li, X.; Hratchian, H. P.; Izmaylov, A. F.; Bloino, J.; Zheng, G.; Sonnenberg, J. L.; Hada, M.; Ehara, M.; Toyota, K.; Fukuda, R.; Hasegawa, J.; Ishida, M.; Nakajima, T.; Honda, Y.; Kitao, O.; Nakai, H.; Vreven, T.; Montgomery, J. A., Jr.; Peralta, J. E.; Ogliaro, F.; Bearpark, M.; Heyd, J. J.; Brothers, E.; Kudin, K. N.; Staroverov, V. N.; Keith, T.; Kobayashi, R.; Normand, J.; Raghavachari, K.; Rendell, A.; Burant, J. C.; Iyengar, S. S.; Tomasi, J.; Cossi, M.; Rega, N.; Millam, J. M.; Klene, M.; Knox, J. E.; Cross, J. B.; Bakken, V.; Adamo, C.; Jaramillo, J.; Gomperts, R.; Stratmann, R. E.; Yazyev, O.; Austin, A. J.; Cammi, R.; Pomelli, C.; Ochterski, J. W.; Martin, R. L.; Morokuma, K.; Zakrzewski, V. G.; Voth, G. A.; Salvador, P.; Dannenberg, J. J.; Dapprich, S.; Daniels, A. D.; Farkas, O.; Foresman, J. B.; Ortiz, J. V.; Cioslowski, J.; Fox, D. J. *Gaussian 09*, Revision B.01; Gaussian, Inc.: Wallingford, CT, 2013.

(26) (a) Perdew, J. P.; Burke, K.; Ernzerhof, M. Generalized Gradient Approximation Made Simple. *Phys. Rev. Lett.* **1996**, 77, 3865–3868. (b) Perdew, J. P.; Burke, K.; Ernzerhof, M. Generalized Gradient Approximation Made Simple. *Phys. Rev. Lett.* **1997**, 78, 1396. (c) Adamo, C.; Barone, V. Toward reliable density functional methods without adjustable parameters: The PBE0 model. *J. Chem. Phys.* **1999**, 110, 6158–6170.

(27) (a) Cancès, E.; Mennucci, B.; Tomasi, J. A new integral equation formalism for the polarizable continuum model: Theoretical background and applications to isotropic and anisotropic dielectrics. *J. Chem. Phys.* **1997**, 107, 3032–3041. (b) Cossi, M.; Barone, V.; Mennucci, B.; Tomasi, J. Ab initio study of ionic solutions by a polarizable continuum dielectric model. *Chem. Phys. Lett.* **1998**, 286, 253–260. (c) Mennucci, B.; Tomasi, J. Continuum solvation models: A new approach to the problem of solute's charge distribution and cavity boundaries. *J. Chem. Phys.* **1997**, 106, 5151–5158.

(28) (a) Dunning, T. H., Jr.; Hay, P. J. In *Modern Theoretical Chemistry*; Schaefer, H. F., III, Ed.; Plenum Press: New York, 1977; Vol. 3, pp 1–28. (b) Dolg, M.; Wedig, U.; Stoll, H.; Preuss, H. Energy-adjusted ab initio pseudopotentials for the first row transition elements. *J. Chem. Phys.* **1987**, 86, 866–72.

(29) (a) Dunning, T. H., Jr. Gaussian basis sets for use in correlated molecular calculations. I. The atoms boron through neon and hydrogen. *J. Chem. Phys.* **1989**, 90, 1007–23. (b) Woon, D. E.; Dunning, T. H., Jr. Gaussian basis sets for use in correlated molecular calculations. III. The atoms aluminum through argon. *J. Chem. Phys.* **1993**, 98, 1358–71.

(30) *CrysAlisPro: Data Collection and Integration Software*, version 1.171.37.35; Agilent Technologies UK Ltd.: Oxford, U.K., 2011.

(31) Sheldrick, G. M. A short history of SHELX. *Acta Crystallogr., Sect. A: Found. Crystallogr.* **2008**, A64, 112–122.

(32) Dolomanov, O. V.; Bourhis, L. J.; Gildea, R. J.; Howard, J. A. K.; Puschmann, H. OLEX2: A complete structure solution, refinement and analysis program. *J. Appl. Crystallogr.* **2009**, 42, 339–341.

(33) MERCURY: (a) Bruno, I. J.; Cole, J. C.; Edgington, P. R.; Kessler, M. K.; Macrae, C. F.; McCabe, P.; Pearson, J.; Taylor, R. New software for searching the Cambridge Structural Database and visualizing crystal structures. *Acta Crystallogr., Sect. B: Struct. Sci.* **2002**, B58, 389–397. (b) Macrae, C. F.; Edgington, P. R.; McCabe, P.; Pidcock, E.; Shields, G.

P.; Taylor, R.; Towler, M.; van de Streek, J. Mercury: visualization and analysis of crystal structures. *J. Appl. Crystallogr.* **2006**, 39, 453–457.